

CSP + PV hybrid solar plants for power and water cogeneration in northern Chile

Carlos Valenzuela^{a,*}, Carlos Mata-Torres^a, José M. Cardemil^b, Rodrigo A. Escobar^a

^a Escuela de Ingeniería, Centro de Energía, Pontificia Universidad Católica de Chile, Vicuña Mackenna 4860, Santiago, Chile

^b Departamento de Ingeniería Mecánica, Facultad de Ciencias Físicas y Matemáticas, Universidad de Chile, Beauchef 851, Santiago, Chile

ARTICLE INFO

Keywords:

CSP + PV
Solar desalination
TRNSYS
Chile

ABSTRACT

The integration between solar energy and seawater desalination is an interesting option in northern Chile due to a high solar potential in the Atacama Desert, where most of the mining operations are located. This industry is intensive in electricity and water consumption; therefore, there is an ideal market opportunity. The CSP + PV plant has the benefits of reduce costs, increase capacity factor and offer high dispatchability, while the integration of a MED plant presents the advantage of using the waste heat. A CSP + PV + MED plant model was performed in TRNSYS implementing a dispatch strategy that prioritize PV output and minimize the turbine shutdowns. The results show that a CSP + PV + MED plant presents a capacity factor 7.6% lower than CSP + PV plant. Regarding the operation of the turbine and the MED plant, the configurations that maximize the operating hours also maximize the performance at partial load, obtaining different PV capacities for the maximum operation hours of the turbine and MED plant. For the CSP + PV + MED plant, different CSP and PV plant configuration between optimal or suboptimal were found to minimize the LCOE and LWC. Also, the best combination between LCOE and LWC is achieved with a CSP close to optimal configuration and suboptimal PV.

1. Introduction

One of the global challenges for humanity in the next years is to reduce greenhouse gas (GHG) emissions with the aim of limiting the global temperature rise (United Nations, 2015). This concern has led in the last decade to rapid growth in renewable energies, which have surpassed coal last year to become the largest source of installed power capacity in the world (IEA, 2016). Solar energy has also followed a noticeable upward trend, e.g., between 2010 and 2014 global solar installed capacity grew 4.5 times (IEA, 2015). Particularly in Chile, the PV capacity increased from 2 MW operating at the end of 2012, to 1,524 MW operating in May 2017. An additional 820 MW are under construction, and 14,840 MW are approved for construction in the environmental evaluation system (CNE, 2017). Investors have seen an opportunity in the country due to an exceptional solar potential, e.g., some places in the Atacama Desert can reach a yearly total about 3,500 kWh/m² of DNI (Direct Normal Irradiation) and more than 300 days of clear skies each year (Escobar et al., 2015).

Another future global challenge is related to water scarcity (United Nations, 2016). Several factors such as increased population, industrial expansion, tourism, and agriculture development have led to increase the water demand in the world. For this reason, some countries mainly

in water-stressed or arid regions are augmenting their freshwater supply with the development of seawater desalination technologies (Ghaffour et al., 2013). Chile, as well as many regions of the planet, is undergoing changes in rainfall that is altering hydrological systems, then this impacts water resources in terms of quantity and quality (Stehr et al., 2010). In addition, the economic development of the country is based on mining, an industry with high water consumption, which makes necessary the search for new water supplies, mainly in the northern region.

Desalination processes require significant quantities of energy (Kalogirou, 2005). Given the global goal of reducing GHG emissions, the latest research efforts are devoted to the implementation of energy minimization strategies and cleaner energy supplies in desalination units (Eltawil et al., 2009; Subramani et al., 2011; Sharon and Reddy, 2015). In particular, the integration between solar energy and seawater desalination is an interesting option in Chile since the lack of freshwater resources occurs near the Atacama Desert, where most of the mining operations are located; therefore, there is an ideal market opportunity to sell electricity and water which requires the design and performance evaluation of solar energy system capable of producing both utilities.

* Corresponding author.

E-mail address: cavalen5@uc.cl (C. Valenzuela).

Nomenclature

| | | | |
|------|-------------------------------|--------|--|
| CF | Capacity Factor | LWC | Levelized Water Cost |
| CNE | Comisión Nacional de Energía | MED | Multi-Effect Distillation |
| CRS | Central Receiver System | MSF | Multi-Stage Flash |
| CSP | Concentrating Solar Power | NREL | National Renewable Energy Laboratories |
| DNI | Direct Normal Irradiation | PV | Photovoltaic |
| FF | Forward Feed | PTC | Parabolic Trough Collector |
| GHG | Greenhouse Gas | RO | Reverse Osmosis |
| GOR | Gain Output Ratio | SAM | System Advisor Model |
| IEA | International Energy Agency | SM | Solar Multiple |
| LCOE | Levelized Cost of Electricity | SWCC | Seawater Cooling Circuit |
| | | TES | Thermal Storage System |
| | | TRNSYS | Transient System Simulation Program |

1.1. Hybrid CSP + PV solar power plants

Owing to its intermittent nature, there is a mismatch between most renewable energy supplies and user demand (Liu et al., 2016). In solar energy, thermal energy storage (TES) is an important research field that follow the aim of overcoming the variability of solar resource. Several TES technologies integrated to concentrating solar power (CSP) plants have been developed in recent years (Gil et al., 2010; Singh et al., 2010). Molten Salt has been indicated as the most feasible and commercial option, but it is still expensive while there is not a significant market penetration of CSP (IEA, 2014). On the other hand, photovoltaic (PV) modules are the cheaper technology today. Moreover, additional cost reductions of 30–50% in PV will lead to global installed capacity of 1,000 GW by 2040 (IEA, 2015). However, PV produce a variable output during the day, developing low capacity factors, e.g., PV solar plants installed in northern Chile have implemented one-axis-tracking in order to increase the capacity factor up to 30% (CIFES, 2016).

CSP + PV hybrid schemes can match PV low costs with high capacity factor (CF), dispatchability and night generation that offer CSP with TES. The CSP + PV concept has been proposed and analyzed through different approaches. Platzer (Platzer, 2014) carried out a study of the performance of a hybrid plant using data for Daggett, California. He analyzed whether the combination of solar thermal power with cheaper photovoltaic systems may present lower levelized cost of electricity (LCOE), and higher dispatchability than either photovoltaics or solar thermal stand-alone power plants. In fact, CSP + PV plants may provide more economical power generation than CSP-only power plants. In addition, using the opportunity to supply electricity during daytime by the PV modules and prioritizing the charging process of the storage (and discharging in low radiation periods), the number of hours dispatching electricity at nominal capacity increased almost 3 times. Another study was done by Green et al. (2015) who assessed the hourly performance of a hybrid plant in Chile through the use of Solar Reserve's SmartDispatch software, where priority levels of plant power output were assigned. This study found that is feasible to achieve capacity factors higher than those achieved by CSP-only plants. Moreover, a PV tilt angle optimized for winter was proposed in order to reduce the seasonality effects.

Parrado et al. (2016) performed an economic study where the LCOE of a hybrid plant in the Atacama Desert by 2050 was calculated. Two scenario projections (Blue Map and Roadmap) made by the International Energy Agency (IEA) were used. The first approach calculated the LCOE for current PV and CSP technologies. The second approach calculated the LCOE for a hybrid plant composed by 20 MW PV and 30 MW CSP. Moreover, economic parameters were projected to estimate the LCOE in 2050. It was found that the LCOE of a hybrid plant tends to LCOE of CSP-only plant or PV-only plant depending on the scenario evaluated and values between 80 and 90 USD/MWh will be achieved by 2050. The last study was developed by Starke et al. (2016) who analyzed the performance of hybrid CSP + PV plants in northern Chile in terms of the LCOE and considering parabolic trough collectors

and central receiver systems. This study concluded that the main advantage of the hybridization of a CSP plant with a PV array is reducing the size of the CSP solar field, achieving CF higher than 80%, and consequently lowering the LCOE.

1.2. CSP + MED integration

Although reverse osmosis (RO) is the most common desalination technology worldwide (Al-Karaghoul and Kazmerski, 2013), thermal desalination technologies are very attractive for combined power and desalination plants. Within thermal technologies, multi-effect distillation (MED) offers the advantages of utilizing low temperature steam as heat source, lower energy consumption compared to multi-stage flash (MSF) and is, so far, the only commercially proven technology that can be operated in part load conditions (Frantz and Seifert, 2015). Regarding CSP integration with desalination, Palenzuela et al. (2011) showed that the integration of a MED plant reduces the cooling requirements of a CSP power plant, but the CSP + RO combination is slightly more efficient. Nevertheless, considering additional factors as environmental constraints and possible limitations of the use of RO, CSP + MED can offer a suitable solution.

Casimiro et al. (2014) carried out a study using a new tool developed in the Transient System Simulation Program (TRNSYS) to simulate the cogeneration of water and electricity, considering a CSP and a forward feed (FF) MED plant. A seawater cooling circuit (SWCC) in parallel to the MED plant was proposed, aiming to operate the MED plant under nominal conditions most of the time, even with a variable heat load output from the steam turbine. It was concluded that coupling CSP + MED/SWCC plants is technically feasible and have the potential to be economically interesting. The electrical performance of the CSP + MED/SWCC is only 5% lower than the CSP alone plant. Palenzuela et al. (2015) presented another study comparing several CSP schemes integrated to MED and RO plants in two locations: Almeria and Abu-Dhabi. Economic parameters as efficiency, LCOE and levelized water cost (LWC) were evaluated. For Abu-Dhabi it was found that CSP + MED presents better performance than CSP + RO, both thermodynamically and economically. In Almeria instead, it was found that CSP + RO is more suitable. Regarding costs, CSP + RO presents a slightly lower LWC, but a higher LCOE than CSP + MED.

Ortega-Delgado et al. (2016) also presented a comparative techno-economic study between MED and RO in Almeria, in order to find the best coupling strategy for a 5 MWe CSP plant. In that context, the best coupling option is with the RO unit connected to the local electric grid, which produces the lower LWC. Finally, Mata-Torres et al. (2017) performed a techno-economic analysis of a CSP parabolic-trough collector (PTC) coupled with a MED plant, in transient conditions, analyzing two configurations and two locations: Venezuela and northern Chile. The results show that the proposed scheme is feasible, and a reduction of 15% of installed cost for northern Chile is observed and 25% for Venezuela. Also, the sensitivity analysis shows that an optimal water cost can be achieved by changing the capacity of the

MED plant in function of the flow extracted from the turbine.

Summarizing, CSP + PV plants may provide high CF's and lower LCOE than CSP-only plants. On the other hand, CSP + MED plants are techno-economic feasible, however depend principally on the irradiation and the specific conditions of each country. Regarding to desalination integrated to a CSP + PV plant, there is a lack of studies. Therefore, the present paper analyzes the feasibility of a CSP + PV + MED scheme aiming to study the effects of the CSP + PV plant operation and how its configuration parameters can affect the operation of the MED plant integration. Several operation modes are proposed in order to simulate different dispatch scenarios. The TES size (in hours), solar multiple (SM) and PV capacity are varied to evaluate technical parameter of operation such as capacity factor and operating hours. An economic analysis is also done in order to obtain an optimal configuration within the simulated cases.

2. System description

In this work, a CSP + PV + MED plant was modeled. The proposed CSP plant is based on a central receiver system (CRS) which was selected over PTC due to its higher operational temperatures and solar to electric conversion efficiency. Also, it represents a commercially proven technology and offers ambitious targets of cost decreasing and technological development in the next years (IRENA, 2012a; Liu et al., 2016). On the other hand, the PV system is composed by several PV arrays, each one coupled to a single inverter. The PV plant is coupled in parallel to the CSP plant, thus the sum of the electricity generated by both plants is delivered to the grid. In addition, a MED plant, which take advantage of residual heat aiming to produce freshwater, is coupled in parallel to the condenser of the Rankine cycle. Fig. 1 presents a schematic layout of the proposal plant.

The CSP model considers a power block of 115 MWe of gross electric power and a two-tank direct TES with a molten salt mixture (60% NaNO₃ and 40% KNO₃). A design temperature of 574 °C for the molten salt loop was selected (NREL, 2013). The power cycle was defined flowing the considerations from (Noureddine et al., 2012; Wagner, 2008). Hence, the Rankine cycle considers two regeneration heat feeders (one high pressure closed feed-water heater and one open feed-water heater or deaerator). The higher design pressure in the Rankine cycle is 100 bars and the condenser pressure is 0.068 bars (baseline case of CSP plant without MED integration). The minimum turbine load is 25% of the gross power (Mitsubishi Heavy Industries, 2007; Balling,

2010; SIEMENS, 2010). The coefficients of heat transfer at the design point for the superheater, evaporator and economizer were calculated according to method developed by Wagner (Wagner, 2008). Regarding operation of the turbine at partial load, the model considers the ellipse law or Stodola's cone law. This law establishes that exists constant relations between mass flow, pressure and temperature despite load changes (Cooke, 1983), which allow to calculate the inlet pressure of each turbine stage. Finally, the heliostat field configuration, the receiver geometry and the tower height was made using the SolarPILOT optimization algorithm, which was used via System Advisor Model (SAM) (Blair et al., 2014). Each heliostat has an area of 144 m² and reflectivity of 95%, but for the model an average reflectivity of 90% was selected, due to the soiling effects in Atacama Desert conditions.

A fixed-angle PV power field was also considered. The PV plant is analogous to the Amanecer Solar project located in northern Chile (KAS Ingeniería, 2012). Therefore the SunEdison MEMC-330 module (SunEdison, 2013) and the Bonfiglioli RPS TL 1460 inverter were considered. The PV system design presents a central inverter configuration, which is commonly used due to its simplicity and low installation cost (Choi et al., 2015). Each inverter, which has a capacity of 1.45 MWdc, is connected to a PV array consisting of 232 strings in parallel and 18 modules per string. The total capacity of the PV plant (in MWdc) can be scaled by increasing the number of inverters. PV modules have a tilt angle equivalent to the latitude (23°) in order to maximize the yearly electricity production. To address the performance of the PV plant in Atacama Desert real conditions, soiling was considered due to that dust accumulation on the PV module surface reduce the glass cover transmittance and hence decreases the amount of solar irradiation reaching the cells (Adinoyi and Said, 2013). There are data about soiling in several PV plants worldwide, but the soiling effect is very specific for each place (Bkayrat, 2013). In the present work, an average soiling of 10% was considered.

The condenser of the Rankine cycle operates at 0.068 bar (CSP plant without MED integration), therefore the condensing temperature is 41.5 °C. This temperature is below the required to operate a MED plant. Thus, it is necessary to limit the turbine output pressure to 0.312 bar (condensing temperature of about 70 °C) in order to allow the integration. The MED plant is designed to condense all the steam coming from the turbine. The MED plant considered in this work is analogous to the Sidem 1 plant, which has a FF configuration with 12 effects and 11 feed heaters (Darwish et al., 2006).

Owing to the transient operation of the system, certain restrictions

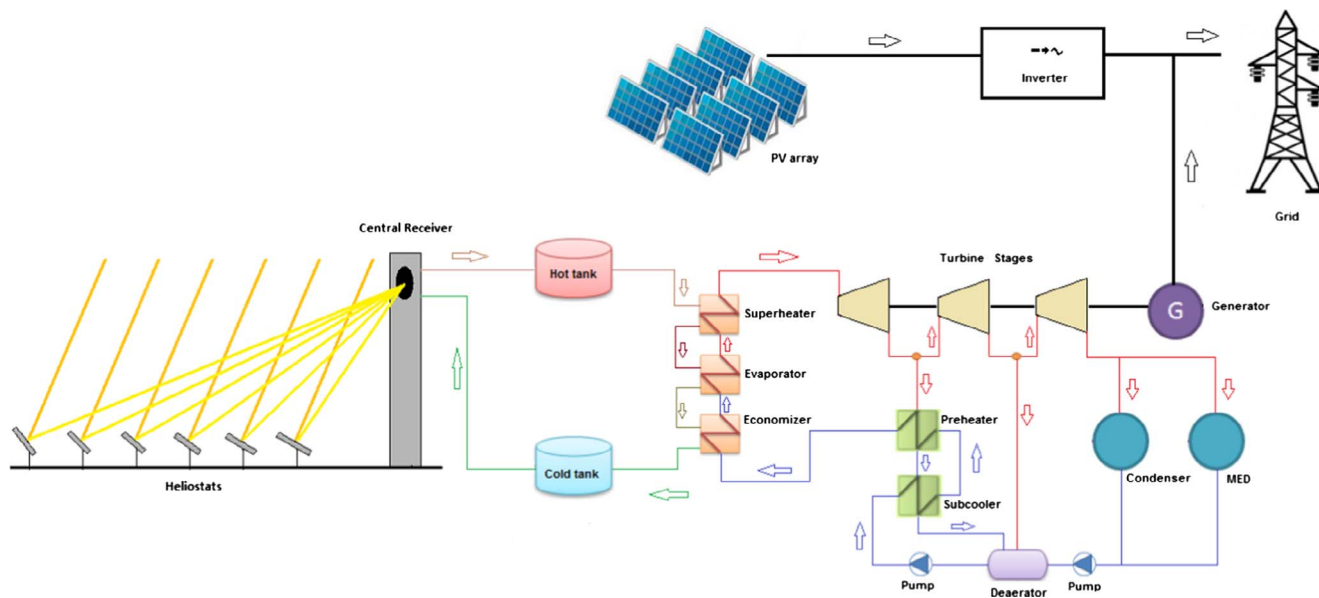


Fig. 1. Scheme of the CSP + PV + MED plant proposed.

were imposed to ensure the smooth operation of the MED plant (Casimiro et al., 2014). A minimum heat load fraction of 50% was implemented. Under this value, the entire steam outlet from the turbine passes through the condenser. When the MED plant is not operating (standby mode), namely temperature and vacuum conditions are preserved since cold startups can take 2h30m in commercial MED plants (Casimiro et al., 2014). Another condition to verify before analyzing the operation of the MED plant is that the inlet steam conditions (pressure and temperature) should be in steady state. The steam condensation pressure is the same for the MED plant and the condenser, even when the MED is in standby mode. Regarding to electric consumption of the MED plant, a specific electricity consumption of 1.5 kWh/m³ was considered (Trieb, 2007). In addition, the seawater pumping consumption from the intake and pumping to the plant was taken into account as a parasitic load of the CSP plant, reducing its gross output.

3. Methodology

The model was performed in TRNSYS (University of Wisconsin-Madison, 2005), where the STEC library components (Schwarzbözl, 2006) were used for modeling CSP plant and the electric library components for the PV plant. The optimization of the heliostat field was made using SAM, where the data obtained were integrated into the TRNSYS model. The plant location was considered in the vicinity of Tocopilla, at 10 km of distance from the sea coast, where the annual DNI is about 3,300 kWh/m² (Solargis, 2017). In addition, in order to perform hourly resolution simulations, the TMY3 data set of Crucero was employed (latitude 22.24° S and longitude 69.51° W). Crucero is located at the same latitude of the locations considered for the hybrid plant, showing annual DNI values of 3,388 kWh/m² (Escobar et al., 2015, 2014). For the configuration described above, the seawater pumping consumption represent 1% of the gross output of the CSP plant. Therefore, for purpose of the present analysis, the elevation of the location was not taken into account, because it leads to some modifications on the model and demands a more detail analysis, as described in the section 5 (Discussion).

The integration between CSP and PV was performed applying a dispatch strategy that prioritizes the PV output and minimizes the turbine shutdowns. CSP power is controlled as a response to the PV output in order to dispatch together a nameplate capacity of 100 MWe; therefore, CSP with TES operate complementing the PV during the day and prioritizing storage, which allows operate a high number of hours at night. On the scenario when the CSP power required to reach the nameplate capacity is less than the minimum turbine load, the turbine generates at minimum load and the surplus PV generation is curtailed depending of the operation mode. The turbine only turns off if the PV power exceeds the nominal power or when the TES is empty. Also, when the TES is at full capacity, the heliostats are defocused for only provide the required energy by power cycle.

To carry out the CSP + PV integration, the parasitic consumption

associated with molten salt pumping between the storage tanks and the receiver, which is located at the top of the tower, was taken from the PV output. This assumption was considered because this consumption occurs only in the day and has a similar profile of the PV generation. The parasitic load from the molten salt pumping between storage tanks and the steam generator, which is in function of the thermal requirement of the power cycle, was taken from the CSP gross output. For the CSP + PV control system, an algorithm that links the net PV output (MWac) with the molten salt flow rate that goes through the steam generator was created. Firstly, the required CSP power is evaluated, and then, the molten salt through the steam generator is calculated.

The MED plant was coupled to the CSP + PV in parallel to the condenser, in order to use the waste heat to drive the desalination process. The steam enters the first effect of the MED, condenses and is reinstated into power cycle. The model of the MED plant was an adaptation of the model described by El-Dessouky and Ettouney (2002), which performed mathematical model at steady state conditions to estimate the GOR. Sidem 1 plant was evaluated by Darwish et al. (2006), Mata-Torres et al. (2017) obtaining a gain output ratio (GOR) of 10.05. In TRNSYS, the behavior of the MED was emulated as a conventional condenser where the heat transfer rate was determined and used as the heat input for the first effect of the MED plant. Then, the freshwater production is assessed by the equation adapted from (Darwish et al., 2006; Mata-Torres et al., 2017), that relates the freshwater production with the heat provided in first effect:

$$D_t = \frac{Q_{med} GOR}{\lambda_s \rho} \tag{1}$$

where D_t is freshwater production in m³/h, Q_{med} is heat transferred in the first effect of MED in kJ/h, GOR is the gain output ratio of the MED model, λ_s is the latent heat at saturation temperature (70 °C) of the drive steam (equal to 2,333 kJ/kg) and ρ is the water density (1,000 kg/m³). The MED plant electric consumption was taken into account as a parasitic load of the CSP plant.

Six operation modes were proposed as shown in Fig. 2. Each operation mode is explained below:

- (A) CSP + PV stand-alone plant with power limit: In this operation mode, the MED plant is off. Therefore, in the Rankine cycle the condenser operates at a pressure of 0.068 bar. The expression “with power limit” means that PV power must be curtailed if the CSP + PV output exceeds the nameplate capacity (100 MWe). This operation mode represents the situation when there are transmission constraints, supply contracts or other factors and the hybrid plant is restricted to dispatch only its nominal power.
- (B) CSP + PV stand-alone plant without power limit: This operation mode is similar than A, but the expression “without power limit” means that all the CSP + PV output can be dispatched. This can happen in Chilean electricity market, since the system operator coordinates the dispatches at minimum marginal cost. Hence, in this

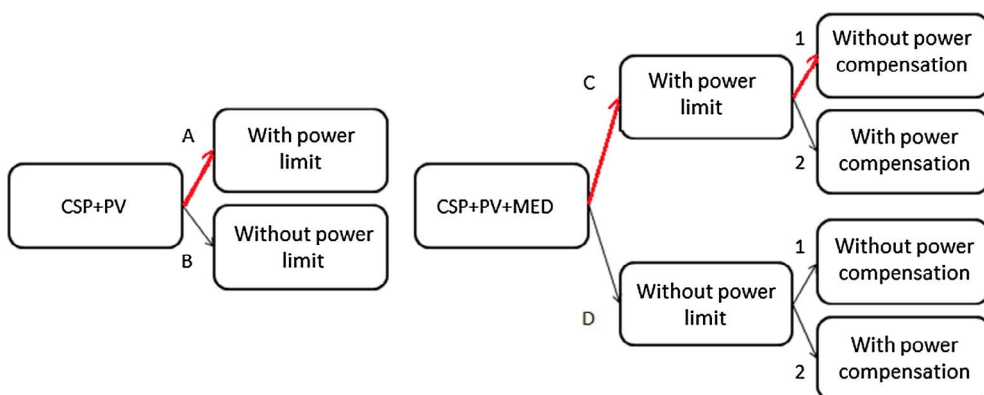


Fig. 2. Operation modes proposed.

scenario PV power should always be dispatched.

- (C1) CSP + PV + MED plant with power limit and without power compensation: In this operation mode and the next ones CSP + PV + MED plant is performed. Therefore, the lower sections of the Rankine cycle presents two streams flowing (through the condenser and the MED plant) as observed in Fig. 1. In that context, the lower pressure of the Rankine cycle is 0.312 bar. The expression “with power limit” has the same means explained before. On the other hand, without power compensation means that the net electricity generation of the turbine decreases (and it is not compensated) due to MED integration.
- (C2) CSP + PV + MED plant with power limit and with power compensation: This operation mode is similar than A, but in order to keep the CSP power output at 100 MWe with the MED on, the power of the turbine is increase in this operation mode, denominated “with power compensation”. To accomplish that, the turbine produces about 120 MWe of gross electric power (within acceptable margins of turbine over design operation) allowing to compensate the drop in net electricity generation due to MED integration
- (D1) CSP + PV + MED plant without power limit and without power compensation: This operation mode is similar to C1, but no power limitation is imposed.
- (D2) CSP + PV + MED plant without power limit and with power compensation: This operation mode is similar to C2, but no power limitation is imposed.

Figs. 3 and 4 show the behavior of the different operation modes using a plant configuration with 140 MWdc PV, 13 h of TES and 1.9 SM. Fig. 3a shows the operation mode B where peaks in the electric power output exist due to the minimization of turbine shutdowns, e.g., in January 2 the turbine does not turn off, but in January 4 the turbine is shut down because the PV power exceeds the nominal power. If the TES is full, this operation mode allows the dispatch of the CSP (January 5 and 6). Fig. 3b shows the operation mode A, where the CSP + PV power does not exceed the nominal power. The PV power is curtailed and if TES is fully charged, the solar field is defocused. Fig. 4a shows the operation mode C1 where the nominal CSP power falls from 100 MWe (Fig. 3) to about 87 MWe. Fig. 4b shows the operation mode C2 where the nominal CSP power is keeping in 100 MWe, but this implies a deeper discharge of the TES, e.g., at the beginning of January 6 the CSP + PV power falls because the TES is empty.

3.1. Economic analysis

To perform the economic analysis, the LCOE and LWC were considered as figure of merit. The LCOE is defined as the cost of electricity

produced by a generator in USD/MWh. As a financial tool, LCOE is very useful for the comparison of different generation technologies. The calculation of the LCOE was performed using the following equation adapted from (IRENA, 2012a; Short et al., 1995):

$$LCOE = \frac{I_{CSP} + I_{PV} + \sum_{t=1}^n \frac{O \& M_{CSP+PVt}}{(1+i)^t}}{\sum_{t=1}^n \frac{E_t}{(1+i)^t}} \quad (2)$$

where I_{CSP} is the initial investment for the CSP plant, I_{PV} is the initial investment for the PV plant, $O \& M_{CSP+PVt}$ are the annual cost considering operation and maintenance plus insurances for CSP and PV, E_t is the annual electricity delivered by the system, i is the discount rate and n is the project lifetime.

The $O \& M_{CSP+PVt}$ costs are decomposed into different items, as shown in the following equation:

$$O \& M_{CSP+PVt} = VC_{CSP} E_{csp_t} + Ins_{CSP} I_{CSP} + FC_{CSP} C_{CSP} + FC_{PV} C_{PV} + Ins_{PV} I_{PV} \quad (3)$$

where VC_{CSP} is the variable cost per generation for the CSP plant, E_{csp_t} is the annual electricity generated for the CSP plant, Ins_{CSP} is the percentage for insurance in the CSP plant, FC_{CSP} is the fixed cost of operation and maintenance for the CSP plant, C_{CSP} is the nameplate capacity of the CSP power block (100 MWe), FC_{PV} is the fixed cost of operation and maintenance for the PV plant, C_{PV} is the capacity of the PV plant in MWdc and Ins_{PV} is the percentage for insurance in the PV plant.

The main economic parameters for the analysis of CSP and PV plants are listed in Table 1. The I_{CSP} value was defined according the information reported in SAM’s cost model, where the cost values for the tower and the receiver are scaled according to the method developed by Gilman et al. (Gilman et al., 2008). The values presented in Table 1 are consistent with the information considered by Starke et al. (Starke et al., 2016). The total CSP installed cost is between 6,153 USD/kW (CRS with SM = 1.5 and TES = 11 h) and 8,251 USD/kW (CRS with SM = 2.3 and TES = 17 h). These values are within the range (3,550 to 8,760 USD/kW) estimated by (Irena, 2015). For the PV plant, the I_{PV} value is in function of the nameplate capacity of the system (MWdc) and the overall installed cost. In the US, the PV system installed cost as of the first quarter of 2016 was around 1.42 USD/W for fixed-tilt utility-scale systems (Fu et al., 2016). In Chile, solar bids about 29 USD/MWh were received in the last electricity tender (Sanchez, 2016), specifically Solar Escondido PV project reported an investment of 290 million dollars by a capacity of 289 MWdc (Golder Associates, 2014), i.e., the PV system installed cost is 1 USD/W, approximately. Hence, for purpose of the present study, the specific installation cost for a PV system was defined as 1.2 USD/W, as a conservative measure.

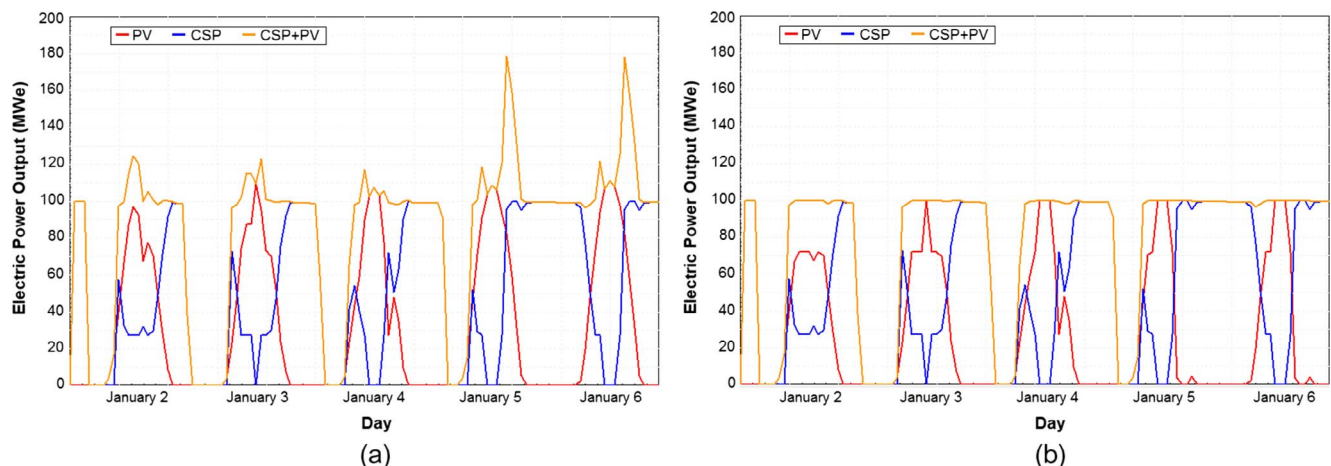


Fig. 3. Operation modes of the CSP + PV plant, (a) operation mode B (b) operation mode A. Configuration simulated: 140 MWdc PV, 13 h of TES and 1.9 SM.

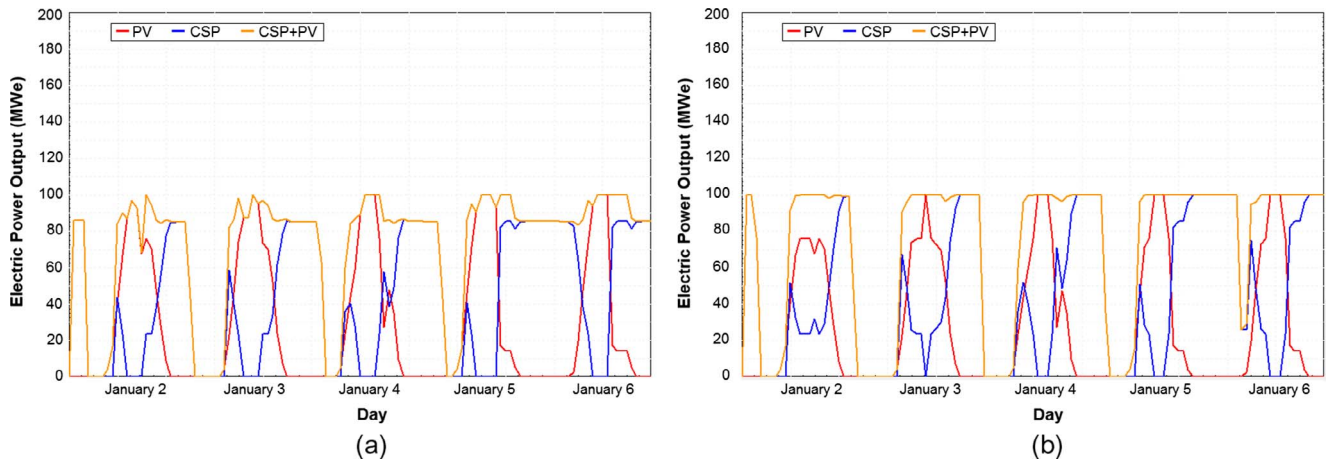


Fig. 4. Operation modes of the CSP + PV + MED plant, (a) operation mode C1 (b) operation mode C2. Configuration simulated: 140 MWdc PV, 13 h of TES and 1.9 SM.

On the other hand, the LWC is defined as the specific cost of water produced in plant's life cycle, expressed in USD/m³. Hence the LWC is defined according the following equation adapted from (Verdier, 2011):

$$LWC = \frac{I_{MED} + \sum_{t=1}^n \frac{O \& M_{MED,t}}{(1+i)^t}}{\sum_{t=1}^n \frac{D_t}{(1+i)^t}} \quad (4)$$

where I_{MED} is the initial investment for the MED plant, $O \& M_{MED,t}$ is the annual cost considering operation and maintenance, D_t is the annual water delivered by the system, i is the discount rate and n is the project lifetime. It should be mentioned that the electric and steam costs of the MED plant were considered as internal costs of the hybrid plant because the waste heat and electric consumption are subtracted from the electricity generation.

The $O \& M_{MED,t}$ costs are composed by the items shown in the following equation:

$$O \& M_{MED,t} = VC_{chemical} D_t + VC_{labour} D_t + FC_{MED} I_{MED} \quad (5)$$

where $VC_{chemical}$ is the variable cost for chemical treatment of water generated, VC_{labour} is the variable cost of operation and maintenance and FC_{MED} is a fixed cost of operation and maintenance that is evaluated

Table 1
Parameters used in the economic analysis with LCOE.

| Plant | Parameter | Value | Unit | Reference |
|---------------------------|--|--------------------|-------------------------------|---|
| CSP | Direct cost: | | | Turchi and Heath (2013) |
| | Site improvements | 15 | USD/m ² heliostats | |
| | Solar field | 170 | USD/m ² heliostats | |
| | Fixed tower cost | 3 | MM USD | |
| | Tower scaling factor | 0.0113 | – | |
| | Receiver reference cost | 110 | MM USD | |
| | Receiver scaling cost | 0.7 | – | |
| | TES | 27 | USD/kWh | |
| | Balance of plant | 350 | USD/kWe (gross) | |
| | Power block | 1,200 | USD/kWe (gross) | |
| | Contingency | 7 | % of direct cost | |
| | Indirect cost: | | | |
| | EPC and owner cost | 11 | % of direct cost | |
| | Land cost | 10,000 | USD/acre | |
| | Sale tax | 0 | % | |
| | Operation and maintenance: | | | |
| | Variable cost (VC_{CSP}) | 4 | USD/MWh | |
| Fixed cost (FC_{CSP}) | 65 | USD/kW (nameplate) | | |
| Degradation rate | 0.2 | % annual | | |
| PV | Fixed cost (FC_{PV}) | 20 | USD/kWdc | U.S. Department of Energy (2012) Jordan and Kurtz (2012), SunEdison (2013) |
| | Degradation rate | 0.7 | % annual | |
| Both | Insurance (Ins_{CSP} and Ins_{PV}) | 0.5 | % of initial investment | U.S. Department of Energy (2012) Short et al. (1995) |
| | Discount rate (i) | 8 | % | |
| | Project lifetime (n) | 25 | years | |

Table 2
Parameters used in the economic analysis with LWC.

| Parameter | Value | Unit | Reference |
|--------------------------------------|------------|-------------------------|---------------------------------|
| <i>Investment costs:</i> | | | |
| Pump station and civil works | 500 | USD/m ³ day | Verdier (2011) |
| Seawater chlorination | 20 | USD/m ³ day | Verdier (2011) |
| Specific cost MED-only plant | 961 | USD/m ³ day | Cipollina et al. (2009) |
| Contingency | 5 | % total cost MED | Verdier (2011) |
| Design capacity of the MED plant | 60,000 | m ³ /day | |
| Initial investment MED (I_{MED}) | 93,303,000 | USD | |
| <i>Operation and maintenance:</i> | | | |
| Fixed cost (FC_{MED}) | 2 | % of initial investment | IRENA (2012b) |
| Chemical ($VC_{chemical}$) | 0.025 | USD/m ³ year | El-Dessouky and Ettouney (2002) |
| Labor (VC_{labour}) | 0.1 | USD/m ³ year | El-Dessouky and Ettouney (2002) |

as a percentage of initial investment. The main economic parameters of the MED plant are presented in Table 2. It is worth mentioning that the overall specific cost for the MED plant (1,481 US/m³) is within the range (800–1,500 USD/m³) estimated by IRENA (2012b).

4. Results and discussion

This section presents a validation of the model and the results of the simulations carried out considering the different operation modes. The results are presented in two different approaches: First to analyze the technical operation and then the minimization of the economic parameters.

4.1. Validation

A validation process was done separately for the CSP, PV, CSP + PV and MED plant. A comparison of the models results with data from real solar power plants, current projects in development or other models found in the literature is shown in Table 3. The CSP model was adjusted to the real conditions of the Gemasolar (NREL, 2013) power plant. This plant has fossil backup that the CSP model not consider; therefore, the comparison was done in terms of the annual electricity generation, disregarding the contribution of the backup system, which is 15% according to the Spanish legislation. The validation of the PV model was performed by comparing the simulation results against operation data from two real plants: Amanecer Solar (KAS Ingeniería, 2012) and DeSoto (Freeman et al., 2013). Amanecer Solar has been in operation since 2014 in northern Chile; its nominal capacity is 100 MWdc and uses SunEdison MEMC-330 modules. DeSoto has been in operation since 2009 in Florida (US); has 27.6 MWdc of nominal capacity and uses SunPower T5-SPR-305 modules. The CSP + PV model was simulated considering available data from Cerro Dominador project, located in northern Chile (Sustentable, 2013). It consists of a CSP plant co-located with a PV plant. The CSP plant consists on CRS with a nominal capacity of 110 MW, while the PV plant has a capacity of 120.8 MWdc, with modules tilted at latitude angle. This solar plant is under construction; therefore, the comparison was done against the of annual electricity generation estimated by the project owner. Finally, the MED model was validated against the results from the Sidem 1 plant, which it has an average freshwater production of 139 kg/s. This latter validation also was done by Darwish et al. (2006). It is worth mentioning that all the variation percentages shown in Table 3 are under 5%.

4.2. Technical operation analysis

4.2.1. CSP + PV and CSP + PV + MED capacity factor analysis

To explore the effect of the PV capacity on the CF of CSP + PV and CSP + PV + MED plants, an analysis for five CSP configurations (defined by TES size and SM) was performed. System outages and maintenance were not taken into account for the estimation of the CF. For this analysis, operation modes A and C1 were considered because they are operation modes with power limit, where a nameplate capacity (100 MWe) is defined and the CF can be calculated. The high CF's observed in Fig. 5 are explained due to the high levels of DNI available in the vicinity of Crucero. Indeed, a CF over 90% can be achieved in

hybrid schemes according to studies carried out in northern Chile (Green et al., 2015; Starke et al., 2016). Fig. 5a shows the results from the simulation of the CSP + PV plant, where the CF surpasses the 80% for configurations with SM's larger than 2.3, independently of the PV capacity installed, while for a 1.5 SM, a CF of 80% is achieved for PV plants larger than 120 MWdc. Fig. 5b shows the results for the CSP + PV + MED plant, where the CF decreases about 7.6% in average, due to the electric consumption of the MED plant, seawater pumping and the reduction in the CSP electricity generation by the increase in the turbine output pressure. Nevertheless, for a 2.3 SM, CF's higher than 70% are achieved, independently of the PV capacity. For PV capacities larger than 100 MWdc, the configurations considering a 1.5 SM also reach capacity factors higher than 70%. It is observed that as the PV capacity increases there is a minor increase of CF for larger SM configurations, and for PV capacities larger than 100–120 MWdc the CF takes an asymptotic, since in that configurations the CSP plant is deactivated in some daylight hours. Moreover, in Fig. 5 it is also observed that the CF is limited by the TES size, since the points considering 11 h of TES develops lower CF's than those considering 17 h of TES.

It is worth mentioning that a configuration with 1.9 SM also is shown in Fig. 5. This represents a non-extreme case which reaches CF's over 90%, when the PV capacity is larger than 100 MWdc. For the CSP + PV + MED plant, the CF developed by this configuration surpasses the 80% at the same PV capacities levels. The configuration considering 1.9 SM and 13 h of TES was selected for analyzing the impact of integrating the MED plant in a CSP + PV plant. The following sections describe an analysis of annual operating hours of the turbine and MED plant, electricity generation and freshwater production.

4.2.2. Annual operating hours analysis

The operating hours of the turbine and the MED plant are used as relevant metrics, in order to analyze the configuration that enhance the operation time of both plants. First, an analysis of a CSP + PV plant is carried out aiming to evaluate the benefit of this integration and then a comparison with the CSP + PV + MED plant is performed. Fig. 6 shows the annual operating hours of the turbine for a CSP + PV plant (operation mode A) considering two different CSP configurations and different PV capacities. Notably, as the PV capacity increases between 0 and 100 MWdc, the operating hours of the turbine increases monotonically. This upward trend is due to the constant operation of the turbine in daylight hours, since up to this PV capacity the CSP plant needs to complement the electricity output. In order to achieve the nominal CSP + PV capacity of 100 MWe. In that context, the hybridization increases the number of hours where the plant is operating using the TES system. It is worth mentioning that the CSP operation as PV backup means that the turbine operates at partial load, reducing its performance. The maximum operating hours of the turbine is achieved for PV capacities around 100 MWdc, however it maximizes the number of hours operating at partial load. For PV capacities larger than 100 MWdc, the operating hours of the turbine decrease. This downward trend is explained since the PV power exceeds 100 MWe and CSP output is not required during some daylight hours. Therefore, the turbine operates mainly during nighttime and is limited by the size of the TES.

From Fig. 6, it is observed that as TES size and SM increase, the operating hours of the turbine also increase. The results show a

Table 3
Validation results.

| Plant | Parameter | Real plant (reference) | Reported value | Model | Variation |
|----------|---|---|----------------|-------|-----------|
| CSP | Annual electricity generation (GWh) | Gemasolar (NREL, 2013) | 110 | – | – |
| | Annual electricity generation without fossil backup (GWh) | | 95.7 | 100.1 | 4.6% |
| PV | Annual electricity generation (GWh) | Amanecer Solar (KAS Ingeniería, 2012) | 270 | 277.3 | 2.7% |
| | | DeSoto (Freeman et al., 2013) | 52.2 | 52.3 | 0.2% |
| CSP + PV | Annual electricity generation (GWh) | Cerro Dominador (Sustentable S.A, 2013) | 950 | 927.9 | -2.3% |
| MED | GOR | Sidem 1 (Darwish et al., 2006) | 9.8 | 10.05 | 2.6% |

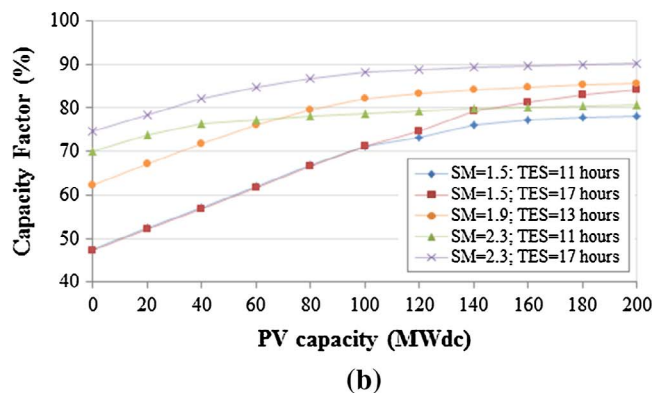
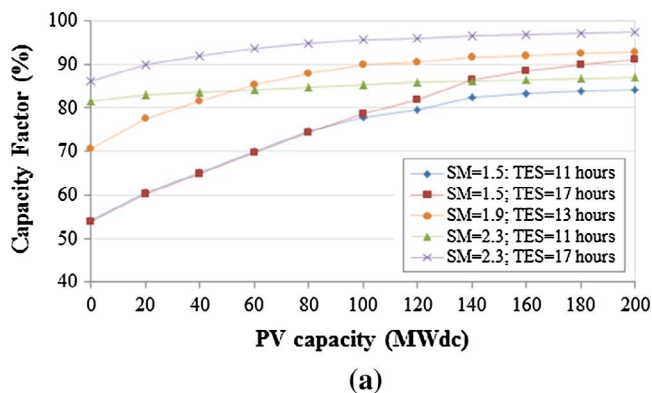


Fig. 5. Capacity factor as a function of the PV capacity for (a) operation mode A and (b) operation mode C1.

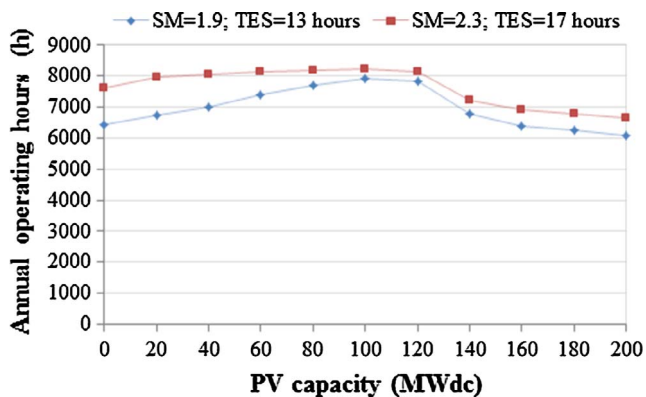


Fig. 6. Annual operating hours of the turbine as a function of the PV capacity for two CSP + PV plants.

maximum of the annual operating hours of 8,030, for a configuration of 1.9 SM and 13 h of TES, and 8,212 h for a 2.3 SM and 17 h of TES. If these results are compared to the annual operating hours of the stand-alone CSP plant reported on Table 4, it can be inferred that the CSP + PV integration reduce the SM and enhance the operating hours of the turbine for a particular TES configuration. Specifically, for 13 h of TES the operation hours increase in 2.9% and for 17 h of TES the operating hours increase in 1.2%.

Fig. 7 shows the operating hours of the turbine and the MED plant for a CSP + PV + MED scheme with 1.9 SM, 13 h of TES and different PV capacities. Fig. 7a shows the results for the operation mode C1 and Fig. 7b shows the results for the operation mode C2. The operating hours of the turbine in the operation mode C1 with the operating hours of the turbine in the operation mode A (Fig. 6) are equivalent. This happens because in the operation mode C1 the MED plant only replaces the function of the condenser in the Rankine cycle; so, the output energy of the turbine is decreased, but the turbine operation hours are not affected.

The trend followed by the operating hours of the MED plant is similar to the trend followed by the turbine; however, the inflection point for the MED plant occurs at smaller PV capacities. For PV capacities from 0 to 60 MWdc the turbine and the MED plant operate almost the same number of hours. At these PV capacities, the turbine contributes to the plant output with more than 50 MWe. Therefore, all the steam coming out of the turbine enters the MED plant, enabling the production of water. When PV capacities ranges from 60 to 120 MWdc the operating hours of the MED plant and the operating hours of the turbine are decoupled, increasing the operating hours of the turbine, while the operating hours of the MED plant decreases. This performance is related to the constraints about minimum flow imposed by the MED plant and the minimum turbine operation. Indeed, when the CSP output range between 30 and 50 MWe the MED plant does not work. For a PV

capacity between 60 and 120 MWdc, is required less than 50 MWe from the CSP output in several daylight hours, therefore during those periods the MED plant does not work. Then, a stabilization on the operating hours of the MED plant is observed for PV capacities from 120 to 200 MWdc, where the turbine reduces its operating hours at partial load because it operates mainly during nighttime; and therefore, the operating hours of the turbine and the MED plant tend to coupled again. It is observed that there is a range in which an increase in the PV capacity increases the operating hours of the turbine and the MED plant, but also increases the operation at partial load. On the other hand, there is other range in which an increase in the PV capacity decreases the operating hours of the turbine and the MED plant, but also increases the operation at full load.

Regarding the operation modes, C2 decreases about 7% in average the operating hours of the turbine and decreases about 8% in average the operating hours of the MED plant, both compared to operation mode C1. However, in terms of number of hours, the reduction is about 485 h in average for the turbine and the MED plant. The operation mode C2 implies mostly full load performance, but it reduces the TES hours available and therefore the annual operating hours. Finally, power compensation generates a tradeoff between operation in over-design point at full load and operation at partial load; both imply an increase in maintenance requirements and overhauls.

4.2.3. Electricity generation analysis

The annual electricity generation as a function of the PV capacity is shown in Figs. 8 and 9. Fig. 8 shows a comparison between results of a CSP + PV plant in operation mode B (Fig.8a) and the CSP + PV + MED plant in operation mode D1 (Fig. 8b). Fig. 9 shows the comparison between operation mode C1 (Fig. 9a) and the operation mode C2 (Fig. 9b). In both figures, it can be observed that an increase in the PV capacity from 60 MWdc, leads to a decrease on the CSP electricity generation. In Fig. 8a with 60 MWdc the CSP electricity generation is 1% lower than a CSP only plant, with 100 MWdc the reduction is about 6% and with 200 MWdc the reduction is about 13%. This situation occurs because there is a combined effect between operating hours of the turbine and partial load operation as described in the previous section. Despite the maximum operating hours of the turbine is achieved for a PV capacity of 100 MWdc, a representative share is due to partial load operation. For the configuration simulated here, a PV capacity of 20 MWdc produce the maximum CSP electricity generation, which is 2% higher than a CSP only plant.

Table 4
Annual operating hours of the turbine in two CSP-only plants.

| | SM = 2.5; TES = 13 h | SM = 2.6; TES = 17 h |
|--------------------------------|----------------------|----------------------|
| Operating hours of the turbine | 7,799 | 8,113 |

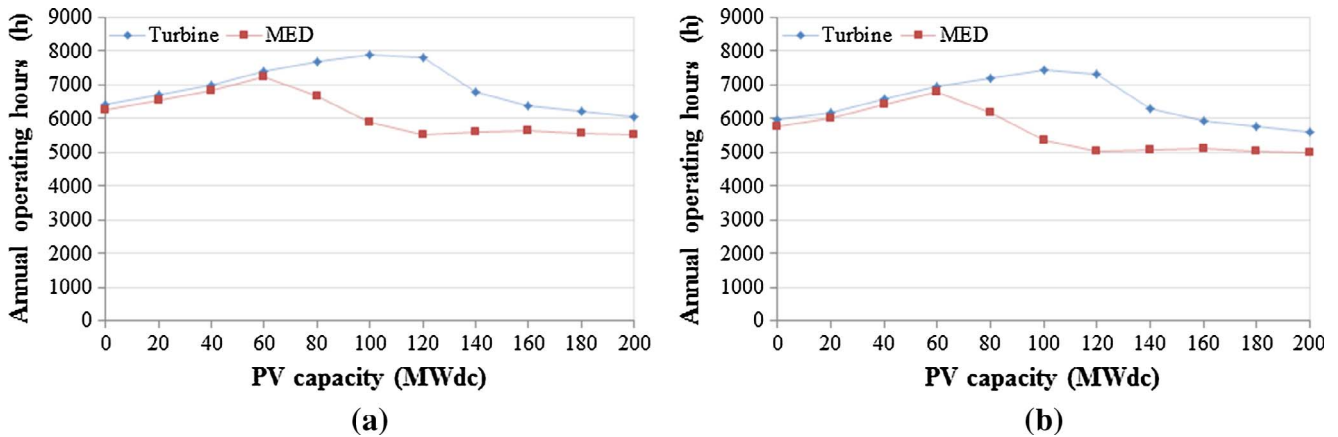


Fig. 7. Annual operating hours of the turbine and the MED plant as a function of the PV capacity for a CSP + PV + MED scheme with 1.9 SM and 13 h of TES (a) operation mode C1 and (b) operation mode C2.

When no power limit is imposed (Fig. 8), the overall electricity generation increases linearly with the PV capacities. Moreover, PV has a larger contribution within the total output as the PV capacity increases, e.g., in Fig. 8a with 200 MWdc, PV provides a 44% of the overall generation, while in Fig. 8b a PV capacity of 200 MWdc, provides a 48% of the overall electricity generation. The comparison between operation modes B and D1 shows that CSP output falls about 14% (average) and PV output remains almost unchanged.

On the other hand, when the electric power output is constraint (Fig. 9), PV generation is curtailed and exist a limit in the annual electricity generation. In this case the PV excess production is dumped, but the CSP output is similar than the D1 case. The comparison between the operation modes shows that C2 has a CSP electricity generation 1% in average higher than C1.

4.2.4. Freshwater production analysis

To analyze the freshwater production profile, the PV capacity was varied, as shown in Fig. 10. The trend depicted is clear, first the annual water production remains constant for PV capacities between 0 and 60 MWdc. Then, a sharp decrease is observed for PV capacities between 60 and 120 MWdc. Finally, the annual water production remains constant for PV capacities larger than 120 MWdc. This trend is in agreement to the observations on the annual operating hours of the MED plant, as previously mentioned. The maximum operating hours of the MED plant is achieved for a PV capacity of 60 MWdc, however a representative share is operation at partial load. The maximum freshwater production is produced when the PV capacity is 40 MWdc PV.

The freshwater production follows the CSP electricity generation, which also achieves its highest level at small PV capacities. Fig. 10 also shows that the power compensation mode operation (C2) produces

slightly less freshwater than the C1 operation mode. This last result complements the previous observations for this operation mode, since the operating hours of the MED plant and the turbine are less than those achieved with the operation mode C1, where the electricity generation is not significantly higher. So, the results shown here and the results of the previous sections say that the power compensation could be not convenient.

4.3. Economic results

In this section, an analysis for the CSP, CSP + PV and CSP + PV + MED plants are presented. First, the LCOE of several stand-alone CSP plants are presented in the Fig. 11, aiming to state a reference value for further comparisons. The results show that the optimal CSP configuration was obtained for a SM of about 2.5 and 14 h of TES, leading to a LCOE of 116.5 USD/MWh. Regarding the PV system, with a PV system installed cost of 1.2 USD/W a minimum LCOE of 68.9 USD/MWh is achieved when the PV tilt angle is equivalent to the latitude.

Fig. 12 shows the LCOE of different CSP + PV plants. A fixed TES size of 13 h was used. Fig. 12a shows the results for the operation mode B and the Fig. 12b shows the results for the operation mode A. It can be observed that without power limit, an increase in the PV capacity over 100 MWdc implies a decrease on the LCOE for any SM. This operation mode does not allow finding an optimum configuration, but the convergence to the LCOE to the PV plant stand-alone is expected. Considering a PV system installed cost of 1.2 USD/W, and PV capacities from 140 MWdc it is possible to achieve lower LCOE than those achieved by stand-alone CSP plants. On the other hand, when power limit is imposed (Fig. 12b) a minimum LCOE can be determined in terms of SM and PV capacity. This happens due to an increase on the PV

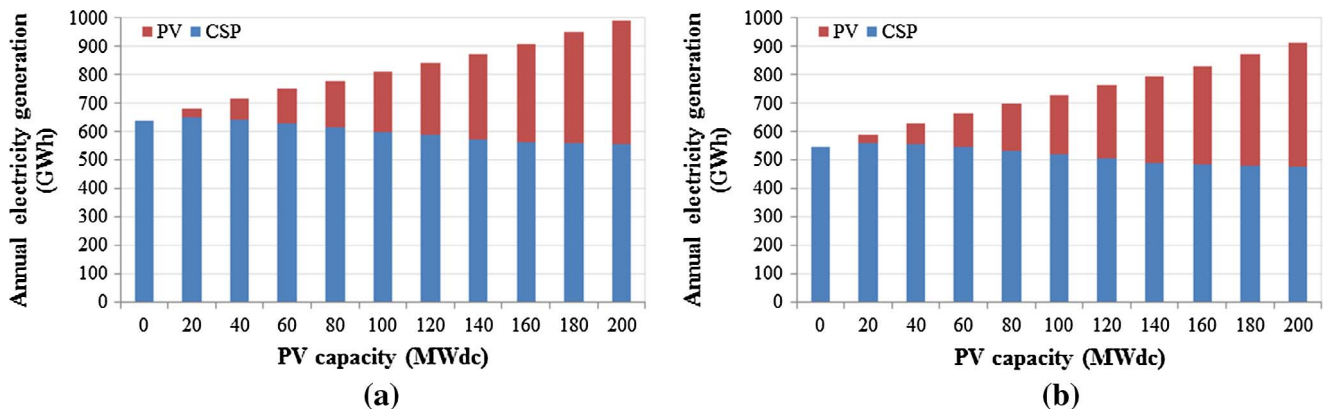


Fig. 8. Annual electricity generation as a function of the PV capacity for (a) operation mode B and (b) operation mode D1.

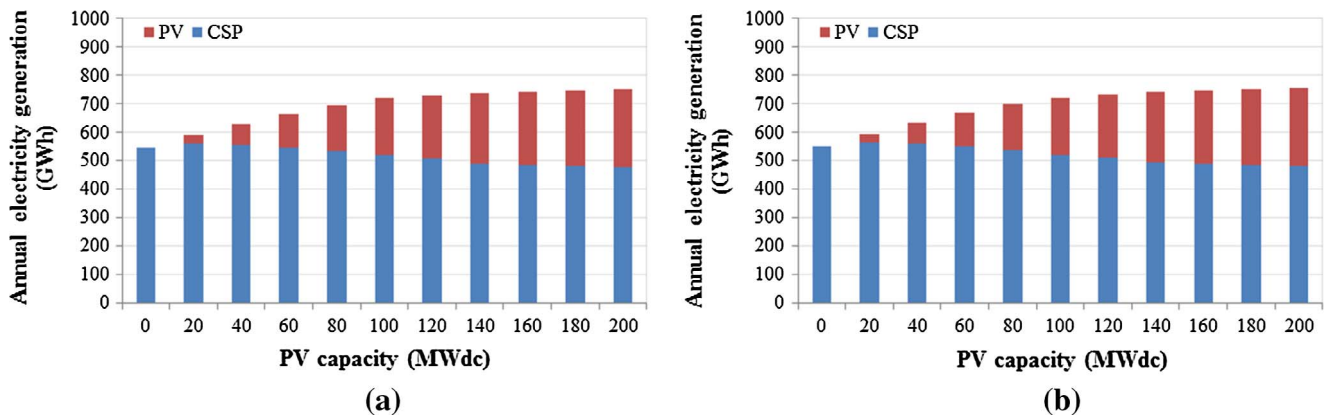


Fig. 9. Annual electricity generation as a function of the PV capacity for (a) operation mode C1 and (b) operation mode C2.

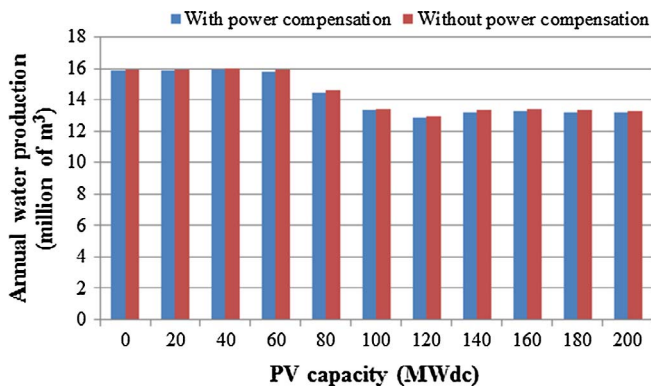


Fig. 10. Annual water production as a function of the PV capacity for two operation modes (C1 and C2).

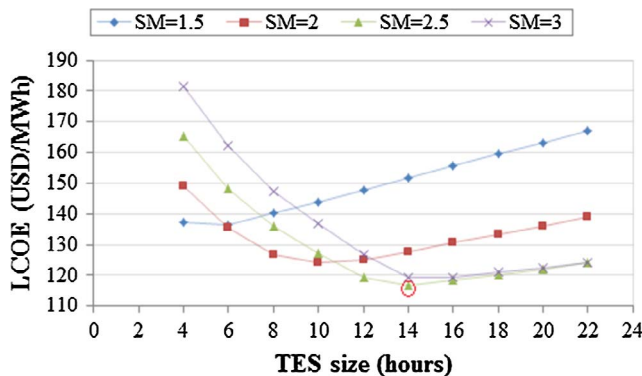


Fig. 11. LCOE of a CSP-only plant as a function of the TES size for several SM.

capacity lead to CSP + PV configurations that uses a suboptimal CSP. Therefore, the LCOE of the CSP plant is higher. Moreover, an increase on the PV capacity from 100 MWdc generate a significant PV power curtailment, therefore an increase in the LCOE of the CSP + PV plant is achieved. From Fig. 12b it inferred that the minimum LCOE occurs for a PV capacity of 20 MWdc and 2.3 SM. Considering a PV system installed cost of 1.2 USD/W, the minimum LCOE achieved is of 116.4 USD/MWh, likewise an optimal CSP plant installed in the same location. However, the CSP + PV configuration's achieve higher CF's.

A comparison analysis varying the PV system installed cost was done, as shown in Fig. 13. It can be observed that with a PV system installed cost of 1.4 USD/W (Fig. 13a) the optimal PV capacity is 0 MWdc. On the other hand, considering a PV system installed cost of 1 USD/W (Fig. 13b) the optimal PV capacity increases up to 80 MWdc, leading to a minimum LCOE of 116.0 USD/MWh. The PV installed cost

is an important parameter since that can change the optimum PV size, although the LCOE do not change notoriously.

To address the economic performance of the CSP + PV + MED plant, the LCOE and the LWC are used as figures of merit. The operation mode C1 and a PV installed cost of 1.2 US/W were considered. Five SM values ranging from 1.5 to 2.3, four TES size ranging from 11 to 17 h and eleven PV capacities ranging from 0 to 200 MWdc were simulated. Fig. 14 shows the results for a TES size of 13 h (Fig. 14a) and 17 h (Fig. 14b). The different colors curves represent PV capacities, the different markers represent SM's and the arrow represent the direction, which the SM increases.

From Fig. 14 it is observed that the lower LWC value is achieved with small PV capacities, between 0–40 MWdc. Also, for each PV capacity the lower LWC is achieved for the large SM, about 2.3. The general trend in the curves shows that for small PV capacities (0–40 MWdc) the LCOE and LWC decrease, as the SM increases. At PV capacities from 80 to 120 MWdc the trend is to achieve a minimum LCOE around SM = 1.9. Finally, with large PV capacities (160–200 MWdc) the LCOE increases alongside with the SM. The comparison between Fig. 14a and b shows the same trend in the curves. However, it highlights that a lower LCOE is obtained with 13 h of TES and the lower LWC is obtained for 17 h of TES.

Fig. 15 shows a scatter plot between LCOE and LWC for all CSP + PV + MED configurations simulated. Four points of interest are highlighted in Fig. 15 and specified in the Table 5. These points represent extreme configurations within the simulated cases.

Table 5 shows that different targets implies different configurations of the CSP + PV + MED plant. First, the minimum LCOE of the CSP + PV + MED plant is 131.2 USD/MWh which provides an increase of 12.7% compared to the minimum LCOE for a CSP + PV plant, besides the benefit of a freshwater production of about 13.4 MM m³/year. Second, if the target is minimizing the LWC, the LCOE increase to 138.3 USD/MWh, however the freshwater production reaches its maximum rate of about 19.3 MM m³/year. The configuration that minimizes the LWC presents a large SM and TES size, but disregard the PV field. This happens because the freshwater production is related to the CSP generation and the hybridization reduces this value. On the other hand, the configuration that minimizes the LCOE present a SM and TES size lower than CSP stand-alone, which is a suboptimal CSP configuration. LCOE minimization also makes use of an intermediate PV capacity, which is optimal because is close to the nameplate capacity of the plant. The 100 MWdc PV capacity also maximize the operating hours of the turbine (see Fig. 7). Other target that can be maximized is the annual electric generation (point 4). In this case, a large SM, TES size and PV capacity are necessary. However, this is a strongly suboptimal configuration for the CSP and PV plants, so the LCOE is higher.

Finally, the configuration that minimizes the LCOE is different to the configuration that minimizes the LWC, as showed before. Between

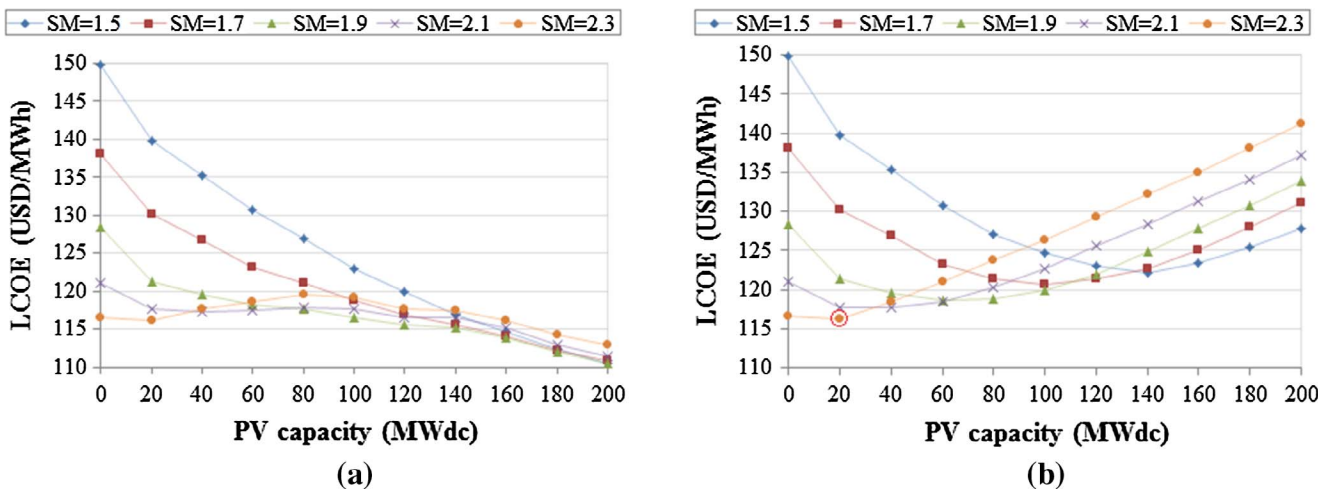


Fig. 12. LCOE as a function of the PV capacity for a CSP + PV plant, (a) operation mode B and (b) operation mode A. The TES size is 13 h and the PV system installed cost is 1.2 USD/W.

them, there are several optimal configurations (see Fig. 15) which adopt a curve shape, resulting in a Pareto curve. Exist a configuration (point 3) that represents the best combination between both economic parameters. This point has a configuration with 40 MWdc, 2.3 SM and 15 h of TES, which is close to the optimal configuration for a CSP standalone plant. Compared to the point 1, this configuration replaced PV capacity with more CSP capacity in order to obtain a higher water production. However, this leads to a suboptimal PV capacity. Notably, the metrics achieved in this configuration are 0.5% higher than the minimum LCOE, and 1.5% higher than the minimum LWC. Nevertheless, the optimum configuration depends on several factors related with the market prices of the electricity and water, technical limitations, demand location and priorities of the plant owner.

5. Discussion

The study of the integration of CSP technology with MED has grown in recent years, showing that these cogeneration plants may represent one of the most feasible options for the future challenges. Its principal characteristic is the advantage of use the thermal energy that is rejected to the environment, improving the rationale energy utilization. However, different problems related to their configuration and modes of operation can be presented. The aim of this work is focused to determine as a first approach the upper bounds of a CSP + PV + MED plant integration, in which the PV plant integration targets to

enhancing the weaknesses of the CSP plant. Different operation modes are proposed and the relevant performance information has revealed. Under the Chilean context, which presents an excellent solar resource potential, the techno-economic feasibility is crucial topic of study. The main result is that different optimal configurations of the plant were estimated in terms of different metrics, but depending on which product is relevant to boost there may be a certain optimum configuration. On the other hand, the addition of the PV plant allows increase the electricity production, nevertheless it increases the number of partial load hours, and can affect the yield of the MED plant depending on the operation mode. The present analysis described several important assumptions that need to be discussed and evaluated in more depth in future works, such as:

- The capacity factor is a metric that allows evaluate the plant performance based on its nominal capacity. However, it may seem not very clear definition when a hybrid solar-solar plant (CSP + PV) is evaluated. It is ambiguous to define a 100 MW CSP + PV plant as two separates 100 MW plants of each technology, which could present a maximum production of 200 MW. It is important to understand that the CF is defined by the expected nameplate capacity and not by the sum of the effective capacity of each plant.
- The seawater pumping consumption and its effects require further analysis, specifically taking into account the location altitude. In the case of northern Chile, this consideration can present a significant

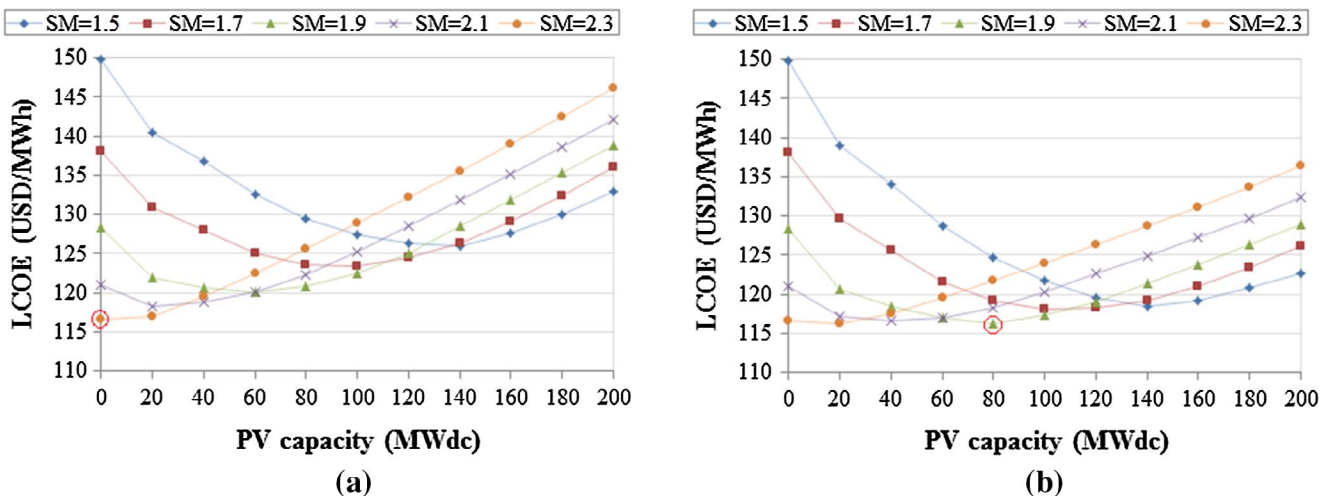


Fig. 13. LCOE as a function of the PV capacity for a CSP + PV plant with operation mode A. TES size is 13 h and the PV system installed cost is (a) 1.4 USD/W and (b) 1 USD/W.

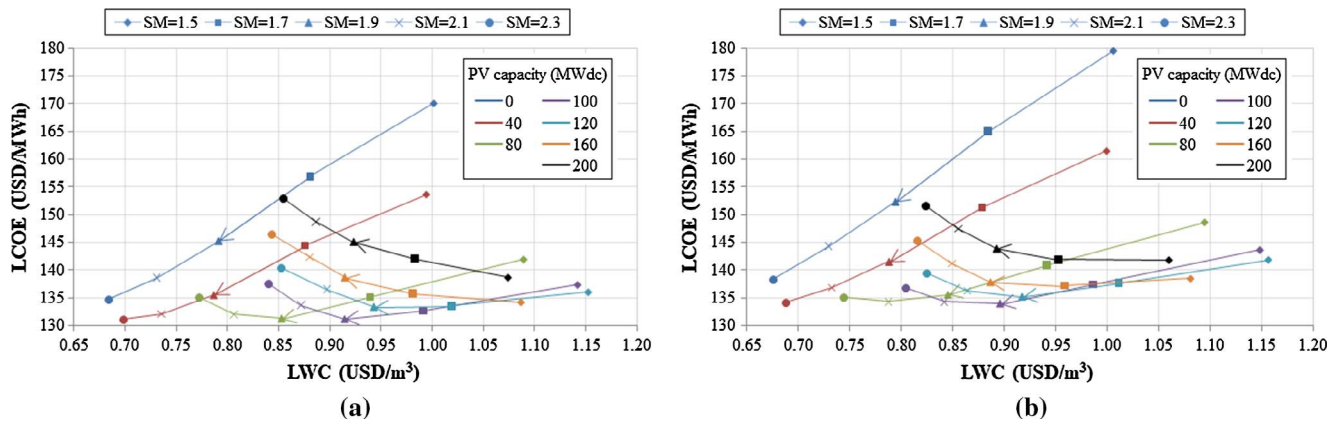


Fig. 14. LCOE versus LWC for different SM and PV capacities keeping the TES size fixed in (a) 13 h and (b) 17 h.

impact because the greater solar resource is at locations higher than 1,000 m.a.s.l. However, it is not a trivial problem to consider, since for 1,000 m altitude the consumption increases to 30% of the electricity production of the CSP plant. This can lead to different operation modes, which are out of the present study scope.

- Soiling must be analyzed for local conditions, in order to considered conditions closer to the real requirements. Also, outages and maintenance schedules must be incorporated.

6. Conclusions

Northern Chile is a place with outstanding irradiation levels, which has generated a great interest for the development of solar energy projects, especially PV due to its low installation cost. However, PV systems generate in a variable profile, a problem that can be mitigated by the adoptions of CSP + PV hybrid schemes. On the other hand, northern Chile has begun to face serious problems of water scarcity which has led to the search for new water supplies. Therefore, a CSP + PV + MED hybrid solar plant for cogeneration of electricity and freshwater was proposed, considering a CRS system of 100 MWe coupled to a MED plant. The complete plant with its several operation modes was simulated in TRNSYS.

The results show that a CSP + PV plant can achieve capacity factors over 80% for all PV capacities and 2.3 SM. The CSP + PV + MED scheme presents a drop of the CF in about 7.6% compared to CSP + PV plant. Also, it has been shown that the maximum operating hours of the turbine is achieved for a PV capacity of 100 MWdc and the maximum operating hours of the MED plant is achieved by a PV capacity of 60 MWdc. However, these sizes also maximize the partial load operation. The CSP + PV integration enhance the operating hours of the turbine for a particular TES size compared to CSP-only plant, but also increase the partial load operation, which can reduce the operating hours of the

MED plant.

The maximum CSP electricity generation and freshwater production occur with small PV capacities, but the maximum overall electricity production occurs at large PV capacities. When the operation mode with power compensation (C2) was considered, a reduction in the operating hours of the turbine and the MED plant was found, compared to the operation mode without power compensation (C1). Although, the operating hours in C2 are mostly full load, this operation mode only generate 1% more of electricity compared to C1. Moreover, C2 produces slightly less freshwater than C1. Power compensation produce an operation in overdesign point and it do not have important benefits in the electricity and water generation, therefore is a not convenient operation mode.

The economic results show that considering a PV system installed cost of 1.2 USD/W and PV capacities from 140 MWdc it is possible to achieve lower LCOE than those achieved by CSP-only plants, when the CSP + PV plant operate without power limit (B). When power limit is imposed (A), a configuration with 2.3 SM, 13 h of TES and 20 MWdc of PV capacity resulted in the configuration that minimize the LCOE of the CSP + PV plant. The LCOE of 116.4 USD/MWh is similar to an optimal CSP-only plant in the same location. It is worth mentioning that a decrease in the PV installed cost can change the optimum PV size, but the LCOE do not change markedly.

On the other hand, a minimum LCOE of 131.2 USD/MWh was achieved for a CSP + PV + MED plant. This value is 12.7% above the minimum LCOE for a CSP + PV plant; however, there is a benefit of 13.4 MM m³ freshwater production. To minimize the LCOE requires intermediate PV capacity due to the lower PV cost. The CSP + PV + MED plant can have different targets depending on which product is relevant to produce. Achieving each target implies different CSP and PV configuration between optimal or not optimal combination, compared to stand-alone plants. Indeed, the minimum LCOE uses a suboptimal

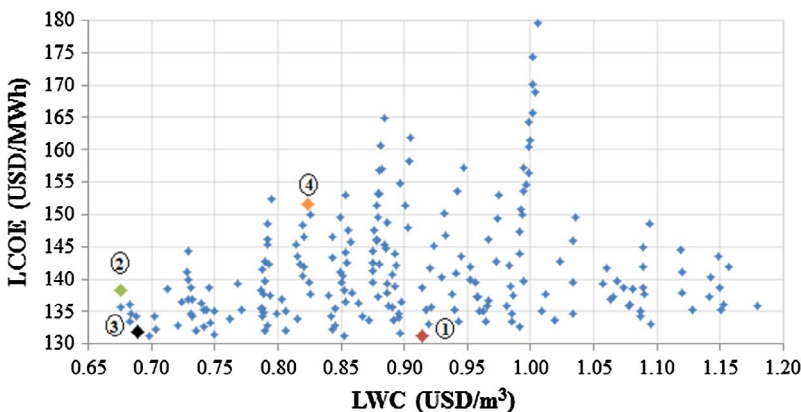


Fig. 15. Scatter plot between LCOE and LWC for several CSP + PV + MED configurations. Operation mode C1.

Table 5

Points of interest and their respective configurations in TES size, SM and PV capacity.

| Point | Characteristic | LCOE (USD/MWh) | LWC (USD/m ³) | Annual electric generation (MWh) | Annual freshwater production (m ³) | TES (h) | SM | PV capacity (MWdc) |
|-------|--|----------------|---------------------------|----------------------------------|--|---------|-----|--------------------|
| 1 | Minimum LCOE | 131.2 | 0.91 | 718,925 | 13,435,860 | 13 | 1.9 | 100 |
| 2 | Minimum LWC and maximum freshwater production | 138.3 | 0.68 | 654,832 | 19,261,386 | 17 | 2.3 | 0 |
| 3 | Best combination between LCOE-LWC within the simulated cases | 131.9 | 0.69 | 718,824 | 18,815,631 | 15 | 2.3 | 40 |
| 4 | Maximum electric generation | 151.7 | 0.82 | 790,561 | 15,183,930 | 17 | 2.3 | 200 |

CSP plant and optimal PV plant. On the other hand, the minimum LWC uses a suboptimal CSP and PV plants. The best combination between LCOE and LWC is achieved with a CSP close to optimal configuration and suboptimal PV, where the LCOE and LWC are close to the minimum values. Resuming, the most suitable CSP + PV + MED configuration depends on several factors such as market prices of the products, technical limitations and priorities of the plant owner.

Acknowledgments

The authors gratefully acknowledge partial financial support provided by project FONDECYT No 1130621.

References

- Adinoyi, M.J., Said, S.A.M., 2013. Effect of dust accumulation on the power outputs of solar photovoltaic modules. *Renew. Energy* 60, 633–636. <http://dx.doi.org/10.1016/j.renene.2013.06.014>.
- Al-Karaghoul, A., Kazmerski, L.L., 2013. Energy consumption and water production cost of conventional and renewable-energy-powered desalination processes. *Renew. Sustain. Energy Rev.* 24, 343–356. <http://dx.doi.org/10.1016/j.rser.2012.12.064>.
- Balling, L., 2010. Flexible future for combined cycle. *Mod. Power Syst.* 61–65.
- Bkayrat, R., 2013. *Lessons Learnt with PV Power Plants in the US Desert*.
- Blair, N., Dobos, A.P., Freeman, J., Neises, T., Wagner, M., Ferguson, T., Gilman, P., Janzou, S., 2014. System Advisor Model, SAM 2014. 1. 14: General Description.
- Casimiro, S., Cardoso, J., Alarcón-padilla, D., Turchi, C., 2014. Modeling multi effect distillation powered by CSP in TRNSYS. *Energy Procedia* 49, 2241–2250. <http://dx.doi.org/10.1016/j.egypro.2014.03.237>.
- Choi, H., Ciobotaru, M., Jang, M., Agelidis, V., 2015. Performance of Medium-Voltage DC-Bus PV system architecture utilizing high-gain DC-DC converter. *IEEE Trans. Sustain. Energy* 6, 464–473.
- CIFES, 2016. *Energías Renovables en el Mercado Eléctrico Chileno Enero 2016*. Santiago, Chile.
- Cipollina, A., Micale, G., Rizzuti, L., 2009. *Seawater Desalination*. Springer.
- CNE, 2017. *Reporte Sector Energético Mayo 2017*. Santiago, Chile.
- Cooke, D.H., 1983. Modeling of Off-design Multistage Turbine Pressures by Stodola's Ellipse.
- Darwish, M.A., Al-Juwayhel, F., Abdulraheim, H.K., 2006. Multi-effect boiling systems from an energy viewpoint. *Desalination* 194, 22–39. <http://dx.doi.org/10.1016/j.desal.2005.08.029>.
- El-Dessouky, H.T., Ettouney, H.M., 2002. *Fundamentals of Salt Water Desalination*.
- Eltawil, M.A., Zhengming, Z., Yuan, L., 2009. A review of renewable energy technologies integrated with desalination systems. *Renew. Sustain. Energy Rev.* 13, 2245–2262. <http://dx.doi.org/10.1016/j.rser.2009.06.011>.
- Escobar, R.A., Cortés, C., Pino, A., Pereira, E.B., Martins, F.R., Cardemil, J.M., 2014. Solar energy resource assessment in Chile: Satellite estimation and ground station measurements. *Renew. Energy* 71, 324–332. <http://dx.doi.org/10.1016/j.renene.2014.05.013>.
- Escobar, R.A., Cortés, C., Pino, A., Salgado, M., Pereira, E.B., Martins, F.R., Boland, J., Cardemil, J.M., 2015. Estimating the potential for solar energy utilization in Chile by satellite-derived data and ground station measurements. *Sol. Energy* 121, 139–151. <http://dx.doi.org/10.1016/j.solener.2015.08.034>.
- Frantz, C., Seifert, B., 2015. Thermal analysis of a multi effect distillation plant powered by a solar tower plant. *Energy Procedia* 69, 1928–1937. <http://dx.doi.org/10.1016/j.egypro.2015.03.190>.
- Freeman, J., Whitmore, J., Kaffine, L., Blair, N., Dobos, A.P., 2013. System Advisor Model: Flat Plate Photovoltaic Performance Modeling Validation Report.
- Fu, R., Chung, D., Lowder, T., Feldman, D., Ardani, K., Margolis, R., 2016. U.S. Solar Photovoltaic System Cost Benchmark: Q1 2016.
- Ghaffour, N., Missimer, T.M., Amy, G.L., 2013. Technical review and evaluation of the economics of water desalination: Current and future challenges for better water supply sustainability. *Desalination* 309, 197–207. <http://dx.doi.org/10.1016/j.desal.2012.10.015>.
- Gil, A., Medrano, M., Martorell, I., Lázaro, A., Dolado, P., Zalva, B., Cabeza, L., 2010. State of the art on high temperature thermal energy storage for power generation. Part 1—Concepts, materials and modellization. *Renew. Sustain. Energy Rev.* 14, 31–55. <http://dx.doi.org/10.1016/j.rser.2009.07.035>.
- Gilman, P., Blair, N., Mehos, M., Christensen, C., 2008. *Solar Advisor Model User Guide for Version 2.0*.
- Golder Associates, 2014. *Declaración de impacto ambiental Proyecto Solar Escondido*. Santiago, Chile.
- Green, A., Diep, C., Dunn, R., Dent, J., 2015. High capacity factor CSP-PV hybrid systems. *Energy Procedia* 69, 2049–2059. <http://dx.doi.org/10.1016/j.egypro.2015.03.218>.
- Hernández-Moro, J., Martínez-Duart, J.M., 2013. Analytical model for solar PV and CSP electricity costs: present LCOE values and their future evolution. *Renew. Sustain. Energy Rev.* 20, 119–132. <http://dx.doi.org/10.1016/j.rser.2012.11.082>.
- IEA, 2016. *Renewable Energy Medium-Term Market Report*. Paris, France.
- IEA, 2015. *World Energy Outlook*. Paris, France.
- IEA, 2014. *Technology Roadmap Solar Thermal Electricity*. <http://dx.doi.org/10.1007/SpringerReference7300>.
- Irena, 2015. *Renewable Power Generation Costs in 2014*.
- IRENA, 2012a. *Renewable Energy Technologies: Cost Analysis Series Concentrating Solar Power*.
- IRENA, 2012b. *Water Desalination Using Renewable Energy Technology Brief*.
- Jordan, D.C., Kurtz, S.R., 2012. Photovoltaic Degradation Rates—An Analytical Review. *Kalogirou, S.A., 2005. Seawater desalination using renewable energy sources. Prog. Energy Combust. Sci.* 31, 242–281. <http://dx.doi.org/10.1016/j.pecc.2005.03.001>.
- Ingeniería, KAS, 2012. *Declaración de Impacto Ambiental Parque Fotovoltaico Llano de Llampos*.
- Liu, M., Tay, N.H.S., Bell, S., Belusko, M., Jacob, R., Will, G., Saman, W., Bruno, F., 2016. Review on concentrating solar power plants and new developments in high temperature thermal energy storage technologies. *Renew. Sustain. Energy Rev.* 53, 1411–1432. <http://dx.doi.org/10.1016/j.rser.2015.09.026>.
- Mata-Torres, C., Escobar, R.A., Cardemil, J.M., Simsek, Y., Matute, J.A., 2017. Solar polygeneration for electricity production and desalination: case studies in Venezuela and northern Chile. *Renew. Energy* 101, 387–398. <http://dx.doi.org/10.1016/j.renene.2016.08.068>.
- Mitsubishi Heavy Industries, 2007. *Tandem Steam Turbine for Cogeneration Power Plant (Optimization for Min. Load Operation)*. Mitsubishi Heavy Ind. Tech. Rev. 44, 4–5.
- Noureddine, Y., Abdalah, K., Kamal, M., 2012. Study of Performance of a Solar Power Tower (15 MW) Simulation and Results. In: *SolarPACES*.
- NREL, 2013. *System Advisor Model (SAM) Case Study: Gemasolar*.
- Ortega-Delgado, B., García-Rodríguez, L., Alarcón-Padilla, D., 2016. Thermoeconomic comparison of integrating seawater desalination processes in a concentrating solar power plant of 5 MWe. *Desalination* 392, 102–117. <http://dx.doi.org/10.1016/j.desal.2016.03.016>.
- Palenzuela, P., Alarcón-Padilla, D.C., Zaragoza, G., Blanco, J., 2015. Comparison between CSP + MED and CSP + RO in Mediterranean Area and MENA Region: Techno-economic Analysis. *Energy Procedia* 69, 1938–1947. <http://dx.doi.org/10.1016/j.egypro.2015.03.192>.
- Palenzuela, P., Zaragoza, G., Alarcón, D., Blanco, J., 2011. Simulation and evaluation of the coupling of desalination units to parabolic-trough solar power plants in the Mediterranean region. *Desalination* 281, 379–387. <http://dx.doi.org/10.1016/j.desal.2011.08.014>.
- Parrado, C., Girard, A., Simon, F., Fuentealba, E., 2016. 2050 LCOE (Levelized Cost of Energy) projection for a hybrid PV (photovoltaic)-CSP (concentrated solar power) plant in the Atacama Desert, Chile. *Energy* 94, 422–430. <http://dx.doi.org/10.1016/j.energy.2015.11.015>.
- Platzer, W., 2014. PV – enhanced solar thermal power. *Energy Procedia* 57, 477–486. <http://dx.doi.org/10.1016/j.egypro.2014.10.201>.
- Sanchez, F., 2016. *Acta Apertura Ofertas Económicas Para Suministro Licitación 2015/01*.
- Schwarzbözl, P., 2006. *A TRNSYS Model Library for Solar Thermal Electric Components (STEC) Reference Manual*.
- Sharon, H., Reddy, K.S., 2015. A review of solar energy driven desalination technologies. *Renew. Sustain. Energy Rev.* 41, 1080–1118. <http://dx.doi.org/10.1016/j.rser.2014.09.002>.
- Short, W., Packey, D.J., Holt, T., 1995. *doi:NREL/TP-462-5173. A Manual for the Economic Evaluation of Energy Efficiency and Renewable Energy Technologies*.
- SIEMENS, 2010. *Steam Turbines for CSP plants*.
- Singh, H., Saini, R.P., Saini, J.S., 2010. A review on packed bed solar energy storage systems. *Renew. Sustain. Energy Rev.* 14, 1059–1069. <http://dx.doi.org/10.1016/j.rser.2009.10.022>.
- Solargis, 2017. *Solargis - iMaps [WWW Document]*.
- Starke, A.R., Cardemil, J.M., Escobar, R.A., Colle, S., 2016. Assessing the performance of hybrid CSP plus PV plants in northern Chile. *Sol. Energy* 138, 88–97. <http://dx.doi.org/10.1016/j.solener.2016.09.006>.

- Stehr, A., Debels, P., Luis, J., 2010. Modelación de la respuesta hidrológica al cambio climático: experiencias de dos cuencas de la zona centro-sur de Chile. *Tecnol. y Ciencias del Agua* 1, 37–58.
- Subramani, A., Badruzzaman, M., Oppenheimer, J., 2011. Energy minimization strategies and renewable energy utilization for desalination: a review. *Water Res.* 45, 1907–1920. <http://dx.doi.org/10.1016/j.watres.2010.12.032>.
- SunEdison, 2013. MEMC SILVANTISTM M330 MODULE.
- Sustentable, S.A., 2013. Declaración de impacto ambiental Planta Solar Cerro Dominador.
- Trieb, F., 2007. Concentrating Solar Power for Seawater Desalination. Stuttgart, Germany.
- Turchi, C.S., Heath, G.A., 2013. Molten Salt Power Tower Cost Model for the System Advisor Model (SAM).
- U.S. Department of Energy, 2012. SunShot Vision Study.
- United Nations, 2016. The United Nations World Water Development Report. Paris, France.
- United Nations, 2015. Framework Convention on Climate Change.
- University of Wisconsin-Madison, 2005. TRNSYS A Transient System Simulation Program.
- Verdier, F., 2011. MENA Regional Water Outlook Part II Desalination Using Renewable Energy.
- Wagner, M.J., 2008. Simulation and Predictive Performance Modeling of Utility-Scale Central Receiver System Power Plants. University of Wisconsin-Madison.